IRIS AperTO

UNIVERSITÀ DEGLI STUDI DI TORINO

AperTO - Archivio Istituzionale Open Access dell'Università di Torino

Fibrinogen enhances the inflammatory response of alveolar macrophages to TiO2, SiO2 and carbon nanomaterials

This is the author's manuscript

Original Citation:

Availability:

This version is available http://hdl.handle.net/2318/1533031 since 2018-12-12T15:32:47Z

Published version:

DOI:10.3109/17435390.2014.978405

Terms of use:

Open Access

Anyone can freely access the full text of works made available as "Open Access". Works made available under a Creative Commons license can be used according to the terms and conditions of said license. Use of all other works requires consent of the right holder (author or publisher) if not exempted from copyright protection by the applicable law.

(Article begins on next page)

20 September 2024

Fibrinogen enhances the inflammatory response of alveolar macrophages to TiO_2, SiO_2 and carbon nanomaterials

Arianna Marucco[a,c§], Elena Gazzano[b,c§], Dario Ghigo[b,c], Emanuele Enrico[d], Ivana Fenoglio [a,c*]

[a] *Dept. Chemistry and NIS – Nanostructured Interfaces and Surfaces, University of Torino, Italy*

[b] *Dept. Oncology, University of Torino, Italy*

[c] *''G. Scansetti'' Interdepartmental Centre for Studies on Asbestos and other Toxic Particulates, University of Torino, Italy*

[d]*Nanofacility, Istituto Nazionale di Ricerca Metrologica (INRIM), Strada delle Cacce 91, I-10135 Torino, Italy.*

[§] These Authors contributed equally to this work.

** Corresponding Author: Ivana Fenoglio, Dept. Chemistry, University of Torino, Italy, via P. Giuria 7, 10125, Torino. e-mail: ivana.fenoglio@unito.it*

Abstract

Many studies have shown that the composition of the protein corona dramatically affects the response of cells to nanomaterials (NMs). However, the role of each single protein is still largely unknown. Fibrinogen (FG), one of the most abundant plasma proteins, is believed to mediate foreign-body reactions. Since this protein is absent in cell media used in *in vitro* toxicological tests the possible FG-mediated effects have not yet been assessed.

Here, the effect of FG on the toxicity of three different kinds of inorganic NMs (carbon, SiO_2 and TiO_2) on alveolar macrophages has been investigated. A set of integrated techniques (UV/vis spectroscopy, DLS and SDS-PAGE electrophoresis) have been used to study the strength and the

kinetics of interaction of FG with the NMs. The inflammatory response of alveolar macrophages (MH-S) exposed to the three NMs associated to fibrinogen has been also investigated. We found that FG significantly enhances the cytotoxicity (LDH leakage) and the inflammatory response (increase of nitric oxide concentration and nitric oxide synthase activation) induced by SiO_2, carbon and TiO_2 NMs on alveolar macrophages. This effect appears related to the amount of fibrinogen interacting with the NMs. In the case of carbon NMs, the activation of fibrinolysis, likely related to the exposure of cryptic sites of FG, was also observed after 24 h. These findings underline the critical role played by FG in the toxic response to NMs.

Keywords:

Fibrinogen, protein corona, clotting, inflammation, macrophages

Introduction

The use of *in vitro* models in alternative to animal tests to assess the hazard of nanomaterials (NMs) is strongly encouraged because of ethical and economical reasons. However, the lack of complexity that characterizes the *in vitro* tests, if compared to *in vivo* conditions, may limit their predictive power. Due to their small dimensions, similar to those of biomolecules, nanoparticles can cross the biological barriers and diffuse in the body through the blood stream (Oberdorster et al. 2005; Pery et al. 2009). This property represents an opportunity in medicine, but it also increases the probability of adverse health effects following the intentional or accidental exposure to NM (Savolainen et al 2010; Schrurs and Lison 2012).

Once in the bloodstream NMs come in contact with plasma proteins. There is a growing body of evidences that proteins govern the fate of NMs in the body and the occurrence of adverse reactions (Lynch et al. 2007, Lynch and Dawson 2008, Lesniak et al. 2012). Several studies focus on the role of serum proteins in the response of cells to NMs (Nagayama et al. 2007, Monteiro-Riviere et al. 2013, Mortensen et al. 2013), while a lower number (Tenzer et al. 2013, Barrán-Berdón et al. 2014)

investigate the role of proteins that are abundant in plasma but absent in serum like fibrinogen (FG) or complement proteins.

FG is a heavy, flexible and elongated protein (47.5 x 9 x 6 nm, 340 kDa), which is mainly synthesized by hepatocytes (Jung et al. 2003), but it may be also secreted by lung epithelial cells in response to inflammatory mediators (Guadiz et al. 1997). Its structure is characterized by two identical subunits, each composed of three polypeptide chains (Aα, Bβ, and γ). FG contains two outer D domains, each connected by a coiled-coil segment to a central E domain. The αC subdomains of D interact with the central domain E.

FG has a net negative charge at physiological pH, mainly owing to the aminoacidic composition of the E region, with an isoelectric point (pI) of 5.5, but the αC subdomains, which are rich in arginine and lysine residues, are positively charged (Jung et al. 2003; Deng et al. 2011).

FG is a polyfunctional protein. It plays a key role in blood clotting, being the precursor of fibrin (Fuss et al. 2001). At the same time it controls the fibrinolytic process (Marder 1982) by activating plasminogen and tissue plasminogen activator (tPA) through binding sites in the αC domains. These sites are cryptic and become exposed during the conversion of FG in fibrin (Tsurupa and Medved 2001; Plow and Hoover-Plow 2004).

FG also participates, with fibronectin, in the stabilization of thrombus by promoting platelet aggregation through RGD binding sites of integrin αIIbβ3 located in the γ chain (Fuss et al. 2001; Jackson 2007). One site in the γ chain, located in the D domain, is responsible for the recruitment of macrophages and leukocytes through the Mac-receptor (Lishko et al. 2002; Tang 1998). FG is, in fact, a ligand for leukocyte integrin $\alpha_M\beta_2$ (Mac-1).

The surfaces of implantable medical devices may adsorb FG. Surface-driven conformational changes may lead to the activation of FG through the exposure of cryptic sites (Lishko et al. 2002; Thevenot et al. 2008). A similar effect was recently reported to occur with NMs (Deng et al. 2011). In the study of Deng and co-workers the NM-induced exposure of the sequence 377-395 in the D-domain of the FG was shown to promote the activation of the integrin receptor Mac-1 of

monocytes, which in turn increases the NF-kB signalling pathway resulting in the release of inflammatory cytokines.

In the present study we investigated the ability of FG to mediate the inflammatory response in MH-S cells, a murine alveolar macrophage cell line that expresses Mac-1 antigen (Mbawuike and Herscowitz 1989), after exposure to three different kinds of NMs, i.e. silica (NM-SiO_2), titania (NM-TiO_2) and carbon (NM-C). These NMs are used in industry in a large range of applications, e.g. as additives in plastic, rubber and paints, or as excipients in drugs, cosmetics and foods. At the same time, they are studied for applications in nanomedicine (Prokop and Davidson 2008).

The MH-S cell line has been selected because macrophages, the first line of defence against inhaled pollutants, play a key role in the inflammatory response through the release of inflammatory mediators such as cytokines, reactive oxygen species and reactive nitrogen species. The release of nitric oxide (NO) associated to the activation of inducible NO synthase (NOS) have been chosen as markers of macrophage activation.

Materials and methods

Nanoparticles. Pyrogenic nanometric anatase/rutile powder (Aeroxide P25) (TiO_2) and pyrogenic nanometric silica powder (Aerosil OX50) (SiO_2) were purchased from Degussa-Evonik (Essen, Germany). The silica surface was cleaned to remove possible adsorbed species by a mild thermal treatment (200°C, vacuum) prior its use. Carbon soot powder (C) was purchased from Sigma Aldrich (St. Louis, MO).

Proteins and reagents. Fetal bovine serum (FBS) and FG (used without further purification) were purchased from Sigma Aldrich. FBS has been deactivated for 30 minutes at 56°C before performing the experiments. In all experiments, ultrapure Milli Q (Millipore, Billerca, MA) water was used. Pre-stained protein molecular weight markers for electrophoresis were purchased from Fermentas (Vilnius Lithuania). All other reagents were from Sigma Aldrich.

The interaction with FG and serum proteins was performed in phosphate-buffered saline (PBS; 0.01 M phosphate buffer: pH 7.4, 0.138 M NaCl and 2.7 mM KCl), a solution simulating the pH and ionic strength of plasma.

Surface Area Measurements. The surface area of the particles was measured by means of the Brunauer, Emmett, and Teller (BET) method based on N_2 adsorption at 77 K (Micrometrics ASAP 2020, Norcross, GA, USA).

Scanning Electron Microscopy/Scanning Transmission Electron Microscopy (SEM/STEM). The scanning electron microscopy (SEM) and scanning transmission electron microscopy (STEM) analysis were acquired in a FEI Inspect F FEG, general purpose SEM equipped with a dual-segment solid state STEM detector for both bright- and dark-field transmission imaging.

Adsorption curves. The powders were suspended (33 mg/ml) in PBS containing FG at different concentrations (0.5-10 g/l). The suspensions were stirred in a thermostatic stirrer at 37°C for 1 h and centrifuged at 11,000 RPM, then filtered through a membrane filter (cellulose acetate, pore diameter 0.45 μm) and the concentration of proteins in the supernatant was determined spectrophotometrically (562 nm) by using the bicinchoninic acid (BCA) assay.

The amount of proteins adsorbed was calculated as difference between the final and the initial concentration of proteins in the supernatant. The results are reported as the mean value of at least three separate determinations ± SEM.

ζ-Potential. The ζ-potential was evaluated by means of electrophoretic light scattering (ELS) (Zetasizer Nano-ZS, Malvern Instruments, Worcestershire, U.K.). In this technique the velocity of particles in an oscillating electric field, which is proportional to their ζ-potential, was measured by

light scattering. The NMs were suspended in PBS and then sonicated for 2 min with a probe sonicator (100 W, 60 kHz, Sonoplus, Bandelin, Berlin, Germany).

The ζ-potential was measured for all the samples in 10 mM PBS at different pH (2−9) obtained by adding HCl or NaOH to the suspension.

The measurements were performed on pristine NMs, NMs incubated with FG (5g/L) and NMs incubated with FG (5g/L) and then washed three times in PBS. The results are reported as the mean value of at least three separate determinations ± SEM.

SDS-PAGE Electrophoresis. 1 mg of each samples was suspended in 1 ml of: a) FG 3.5 g/l; b) FBS (0.8 g/l); c) FBS (0.8 g/l) and FG (3.5 g/l); in 10 mM PBS. The suspensions were stirred in a thermostatic stirrer at 37°C for 1 h or for 24 h and centrifuged at 11,000 RPM, then filtered through a membrane filter (cellulose acetate, pore diameter 0.45 µm). Thirty µl of supernatant were collected and processed in reducing Laemmli solution (10µl), heated at 95°C for 5 min. The aliquots of supernatants (10 µl) as well as the protein marker (5µl) were loaded on 8% sodium dodecyl sulphate-polyacrylamide gels (SDS-PAGE). After the separation (105 V, 400 mA for 90 min) the gels were stained in Coomassie staining solution (0.25 % w/v Coomassie R-250 in methanol : acetic acid : water 4:1:5) for 5 min under stirring and de-stained (methanol : acetic acid : water 4:1:5) for 2 h.

Cells and cell medium. Murine alveolar macrophages (MH-S) were provided by Istituto Zooprofilattico Sperimentale “Bruno Ubertini” (Brescia, Italy). Cells were cultured in 100 mm-diameter Petri dishes in RPMI-1640 (Gibco, Paisley, UK) supplemented with 10% FBS up to 90% confluence and then incubated in the same culture medium for 24 h in the presence of the powders. The protein content of the cell monolayers was assessed with the BCA kit.

NMs dispersion in cell medium. The powders were suspended in cell medium and diluted at the final concentration (10 and 50 μg/ml). The suspensions were sonicated twice for 5 seconds at 24% of the power with a probe sonicator (100 W, 20 kHz, Sonoplus, Bandelin, Berlin, Germany). The stability of the suspensions was evaluated by dynamic light scattering (DLS, Zetasizer Nano-ZS, Malvern Instruments, Worcestershire, U.K.). All cells tests were performed with the pristine powder and with the powders pre-incubated (0.1 mg/ml) with buffered solutions of FG at three different concentrations (0.75, 3.5 and 10 g/l). To assess if the effects were due to native FG eventually detached from the NMs surface or FG associated to NMs, FG at a concentration of 1 mg/ml in cell medium was used as control.

Lactate Dehydrogenase (LDH) Activity. The cytotoxic effect of NMs was measured as leakage of LDH activity into the extracellular medium as previously described (Polimeni et al. 2008) with a Synergy HT microplate reader (Bio-Tek Instruments, Winooski, VT). Extracellular LDH activity (LDH out) was calculated as percentage of the total (LDH tot = intracellular + extracellular) LDH activity in the dish.

NO release. After a 24 h incubation, the extracellular medium was removed, centrifuged at 13,000 x g for 60 min, and tested for the content of nitrite, which is a stable derivative of NO, using the Griess method as previously described (Ghigo et al. 1998). The amount of nitrite was corrected for the content of cell proteins and results were expressed as nmol/mg cellular proteins

NO Synthase (NOS) Activity. After a 24 h incubation, the NOS activity was measured with the Ultrasensitive Colorimetric Assay for Nitric Oxide Synthase kit (Oxford Biomedical Research, Oxford, MI) according to the manufacturer's instructions. Results were expressed as nmol nitrite/min/mg cellular proteins.

Statistical Analysis. All data in text and figures are provided as means ± SEM. Results were analyzed by a one-way analysis of variance (ANOVA) followed by Tukey's posthoc test (software: SPSS 19.0 for Windows, SPSS Inc., Chicago, IL). $p < 0.05$ was considered significant.

Results

Properties of the materials. The three NMs chosen for the present study are highly pure and have a similar specific surface area (Table 1). All samples are formed by aggregates of nanoparticles. However, the Secondary Electrons SEM analysis (Figure 1) revealed differences in morphology at a nanometric level. A narrow size distribution of the primary particles was found for NM-TiO_2 while NM-SiO_2 exhibited particles of different sizes. However, in both cases, the mean size of the particles (Table 1) was in the same range, and similar to the longest dimension of FG. In the case of NM-C the primary particles were sintered each other to form chain-like structures. The presence of steps and edges makes the surface of this material rough. The comparison of the micrographs obtained in SEM and STEM bright-field modality (Figure S1, SI) further confirm the irregular structure of this material. The surface chemistry of the three NMs is obviously very different. Silica is a covalent solid exposing at the surface weakly acidic hydroxyl groups while titania is amphoteric ionic oxide exhibiting Brønsted acidic functionalities (Ti-OH) and Lewis acid centres (Ti^{4+}), whose relative abundance depends on pH. While elemental carbon is intrinsically hydrophobic, the graphitic carbon NM used here, which has been made by combustion, is partially oxygenated at the surface and exposes acidic hydroxyl or carboxyl groups. Therefore, like titania and silica, these particles are expected to be charged in water. The surface charge density of a particle at a given pH and ionic strength may be indirectly evaluated by measuring the ζ-potential (Fenoglio et al. 2011). In the present case it has been measured in saline phosphate buffer (PBS), a medium having the same ionic strength and pH of plasma (Table 1 and Figure S2, SI).

At pH 7.4 the values of the ζ-potential were similar for NM-TiO_2 and NM-SiO_2 (-30, -35 mV) while NM-C exhibited a slightly lower value (-23 mV), in agreement with the lower abundance of Brønsted acidic surface functionalities (Table 1).

Fibrinogen- NMs interaction. The powders were incubated for 1 h in PBS at pH 7.4 containing 0.5 to 10 g/l of FG, thus including the physiological concentration range in human blood (1.8-3.5 g/l) (Karmali and Simberg 2011). Bovine plasma FG was chosen as model for human fibrinogen since it has a high sequence homology with the human and the murine type. In fact, no heterologous foreign protein reaction *in vivo* was observed (Tang 1998; Doolittle 2003).

The amount of FG per surface unit adsorbed on the NMs versus the free protein concentration at equilibrium is reported in Figure 2A. A very different trend of the curves is observed for the three samples. In the case of NM-C the amount of FG adsorbed slowly increases by increasing the applied concentration and the curve reaches a plateau at a value corresponding to the one theoretically necessary to form a uniform layer of protein adsorbed in the native conformation side-on (horizontal line). Conversely, FG appears to bind in very high amounts to NM-TiO_2 and NM-SiO_2 even at low concentration, reaching values higher than the side-on theoretical monolayer. At protein concentration in the range of the physiological one (vertical lines), differences were observed also between the silica and titania NMs, being silica the material able to interact with the highest amount of protein. Due to the tendency of FG to self-assembly (Koo et al. 2010; Marucco et al. 2014), a high amount of FG interacting with the NMs does not necessarily correspond to the full coverage of the surface. An estimation of the extent of surface coverage by the protein may be obtained by measuring the isoelectric point (IP) shift of the NMs following the progressive increase of the applied protein concentration (Rezwan et al. 2005; Turci et al. 2010). The IP of a NM completely coated by a protein is expected to be close to the IP of the protein. In the present case a shift of IP toward the protein IP is observed for all samples (Figure 2B and S2, SI) but even at a concentration corresponding to the last point of the adsorption isotherms (10 g/l) the IP of the

protein was not reached for any sample, suggesting that FG does not cover completely the surface or, alternatively, that the molecules preferably arrange at the surface with the more positive domains toward the solution/nanoparticles interface.

To investigate the strength of the interaction established between FG molecules and the three kind of NMs, the FG-NM conjugates were incubated in PBS, thus applying a negative concentration gradient, and the ζ-potential as a function of pH of the surface was evaluated immediately after re-suspending the particles in PBS, according to a protocol previously described (Turci et al. 2010). For NM-TiO_2 no shift of the ζ-potential was observed even after three subsequent incubations in PBS (figure 3A and Figure S3, SI), suggesting that FG interacts irreversibly with this material. A slight reversibility was observed for NM-SiO_2, while in the case of the NM-C a dramatic shift of the ζ-potential was observed (Figure 3A and Figure S3, SI). However, also in the case of NM-C, the ζ-potential after three washings was still different from those of the pristine material, thus suggesting that a fraction of the FG molecules remains tightly adsorbed.

The reversibility observed for the NM-C may be due to both thermodynamic and kinetic reasons. To discriminate among the two factors, the experiments were repeated on this material after 24 h of incubation with FG. The amount of FG adsorbed (Figure 2A) and the extent of coverage (Figure 2B) largely increased by respect to what observed at 1 h, suggesting that the protein corona around this kind of NM requires a long time to reach a thermodynamic equilibrium. On the other hand, after 24 h the interaction appears to be still partially reversible (Figure 3A and Figure S3, SI).

These findings were confirmed by SDS-PAGE electrophoresis (Figure 3B). After 1 h, the NMs decreased the concentration of FG in the supernatant in the order NM-SiO_2>NM-TiO_2>>NM-C. After 24 h, while the affinity of silica and titania for the serum proteins appeared quite similar to those observed after 1 h, the band of FG in the solution incubated with NM-C disappeared, confirming the low rate that characterizes this process.

Fibrinogen- NMs interaction in the presence of serum proteins. To investigate the behaviour of FG in competitive conditions, the NMs were incubated with a solution containing FG and serum proteins at physiological concentration for 1 and 24 h, then the powders were eliminated by centrifugation, and the supernatant analyzed by SDS-PAGE electrophoresis (Figure 3B). Serum proteins decreased the amount of FG interacting with NM-SiO_2 and NM-TiO_2 after 1 h, but didn't completely replace it. This was expected since FG interacts strongly with NM-SiO_2 and NM-TiO_2. Furthermore, the protein-corona evolved and after 24 h the intensity of the FG band slightly increased suggesting that in the serum protein pool other proteins exhibited a high affinity for the NMs surface. Due to the weakness of the interaction of FG with NM-C the replacement of FG with other serum proteins was expected after 24 h. However, interestingly, in the case of NM-C a different process was observed: after 24 h the bands corresponding to the Aα and Bβ chains of FG in the supernatant disappeared, but not those of the γ chain, suggesting that the degradation of FG occurs. The SDS-PAGE analysis of the proteins interacting with NM-C (Figure S4, SI) showed that Aα and Bβ chains remain adsorbed at the NM surface.

Inflammatory response of macrophages exposed to FG/NM conjugates. To investigate the role of adsorbed FG in the response of macrophages to NMs, an alveolar macrophage cell line (MH-S) was treated with the NMs, alone or with the NMs pre-incubated with FG (10 g/l) for 1 h (Figure 4), at two different doses (10 and 50 μg/ml, which correspond to 2 and 10 μg/cm^2, respectively) and the release of lactate dehydrogenase (LDH) from the cells, a sensitive index of loss of membrane integrity, was measured. Only pristine silica exhibited a cytotoxic effect at all doses applied in the absence of FG. When pre-incubated with FG, NM-SiO_2 maintained its high cytotoxicity, but a significant cytotoxic effect was observed also for both NM-C and NM-TiO_2 (Figure 4A). When the ability of macrophages to synthesize NO, a marker of inflammatory response, was measured in terms of both nitrite concentrations in the extracellular medium (Figure 4B) and intracellular NOS activity (Figure 4C), we observed that, contrary to pristine NMs, all three FG-treated NMs induced

a significant increase of NO and of the enzyme responsible for its synthesis. The lipopolysaccharide (LPS) was used as a positive control of inflammatory response: it caused an increased cytotoxic effect and stimulated NO synthesis (Figure 4).

To clarify if the observed effects were due to adsorbed FG or FG eventually detached from the surface during the incubation, and to exclude heterologous foreign protein reactions, the experiments were also performed in the presence of soluble FG (1 mg/l). In this case no increase of NO release and NOS activation was observed compared to pristine NMs, confirming that the interaction with the NM is necessary for the observed FG-mediated inflammatory response (Figure 4). The experiments have been also repeated by pre-incubating the powders with different concentrations of FG (0.75, 3.5 and 10 g/l, Figure 5) to evaluate if the extent of coverage of the surface would affect the FG-mediated response (Figure 5). A toxic and inflammatory response was observed only with NMs pre-incubated with FG at the two highest concentrations. Even in this set of experiments LPS was a positive inducer of NO synthesis and cytotoxicity, and FG alone was devoid of any effect (Figure 5).

Discussion

The concept of "protein corona" is widely used to indicate the dynamic layer of proteins associated to NMs in biofluids (Lynch et al. 2007, Lynch and Dawson 2008). A growing number of studies have demonstrated that the protein corona plays a key role in the response of cells to NMs (Gunawan et al 2014). Recently, Tenzer and co-workers showed that the pre-incubation of NMs with human plasma affects the nanoparticle uptake and the cytotoxicity of NM in endothelial cells (Tenzer et al 2013). Several plasma proteins are known to mediate adverse responses of cells to biomaterials, among them fibrinogen, immunoglobulins and complement proteins (Thevenot et al. 2008, Deng et al. 2011, Engberg et al. 2012). However, the molecular mechanisms underlying these effects are still poorly known.

Here we demonstrate that fibrinogen associated to NMs mediates the inflammatory response of alveolar macrophages to NMs.

Three highly pure TiO_2, SiO_2 and carbon NMs having very similar specific surface area and structure were chosen for this study (Table 1). FG interacts in high amount and irreversibly with TiO_2 and SiO_2, while the interaction with the carbon NM appears partially reversible. A different behaviour was expected because of the different kind and abundance of surface sites able to interact with the protein (Norde 2008, Fenoglio et al. 2011). Protein relaxation, entropically more favourable on hydrophobic surfaces is one of the factors that contribute to the irreversibility of protein adsorption (Fenoglio et al. 2011). Therefore, FG was expected here to interact more strongly with NM-C, that exhibit hydrophobic patches at the surface. Reasons of the anomalous behaviour of FG may be found on the irregular surface of NM-C (Figure 1), the roughness of which at a nanometric scale may act as a steric barrier against FG, as observed in biomaterials functionalized with polymers (Owens and Peppas 2006). Note however that the reversibility is only partial, since some FG molecules remain irreversibly adsorbed at the surface, possibly as a consequence of the morphological heterogeneity of this material.

The adsorption of blood proteins onto an inorganic surface implies competition between thousands of different proteins for the adsorption sites. During this process, that has been described firstly by Leo Vroman in 1962 (Vroman 1962), the proteins with higher mobility adsorb first and are subsequently replaced by less motile proteins with a higher affinity for the surface (Vilaseca et al. 2013). Both kinetic and thermodynamic factors are important since the process may take several h to get to equilibrium (Galisteo and Norde 1995). FG is a high molecular weight protein and therefore is expected to have a low rate of diffusion. However, it may replace other proteins depending upon its affinity for the surface. In the present case, FG interacts, albeit in different amount, with the three NMs also in the presence of other serum proteins. This finding is in agreement with several previous studies that report a high affinity of FG for surfaces (Wertz and Santore 2002, Ruh et al. 2012) of very different nature like graphene (Mao et al. 2013), lipid NMs

(Barrán-Berdón et al. 2013, Pozzi et al. 2014), silica (Tenzer et al. 2013) and polystyrene (Lundqvist et al. 2008, Tenzer et al. 2013).

FG clearly enhances the ability of the three NMs to induce an inflammatory response measured as NO release and NOS activation (Figures 4). While extracellular nitrite is an index of the actual NO synthesis during the in vitro incubation with different stimuli, the intracellular NOS activity, measured on the cell lysate in the presence of saturating substrate concentrations (Vmax) is an index of the increased amount of the enzyme content, as a consequence of the inflammatory reaction. Furthermore, an increase of cytotoxicity in the presence of FG was observed for NM-TiO_2 and NM-C. Since native FG had no effect we assume that the interaction with NMs induces in FG conformational changes leading to the exposure of cryptic sites, able to bind and activate the integrin $\alpha_M\beta_2$ (Mac-1) receptor, as previously observed by Deng and co-workers (Deng et al 2011), that increases the NF-kB signalling pathway and, in turn, induces the activation of NOS. By comparing Figure 2 and Figure 5 is possible to state that these effects are observed only if the amount of FG interacting with the NMs is equal or above the one necessary to form a theoretical monolayer, suggesting that the exposure of the cryptic sites is switched by the interaction among protein molecules at the surface.

In the case of NM-C the activation of the fibrinolytic process was observed after 24 h. This likely occurs through the surface-driven exposure of the cryptic binding sites for plasminogen and t-PA activator in the αC domains of FG (Tsurupa and Medved 2001; Tsurupa et al. 2009) which in turn initiate fibrinolysis. This mechanism mimics the exposure of these sites that occurs after the conversion of FG to fibrin during clotting (Tsurupa and Medved 2001). The FG degradation occurs through different steps that involve, firstly, the cleavage of Aα polar appendices and of Bβ chains, and secondly the cleavage of the γ chain (Fuss et al. 2001). In the present case, Aα and Bβ chains, that are positively charged, remained totally adsorbed at the negatively charged surface, while the external γ chain, having a net negative charge, was found also in the supernatant. The activation of the fibrinolytic process occurs in NM-C but not on silica and titania. This may be related to

different arrangement of FG interacting with the three NMs. It is worth of note that coagulation or FG self-assembly was reported to be induced by NMs of different chemical nature (Jones et al. 2012; Marucco et al. 2014) suggesting that NMs are able to interfere with the coagulation system in different ways depending upon their properties.

Conclusions

The present data clearly show that fibrinogen plays a pivotal role in the inflammatory response of macrophages to silica, titania and carbon NMs. The effect appears switched by a cooperative interaction of fibrinogen molecules with the NM surface. The activation of the fibrinolytic process was also observed after 24h only for the carbon NMs suggesting a specificity of the fibrinogen arrangement at the surface that depends upon NM physico-chemical properties.

Taken together these data suggest that the absence of fibrinogen in the pool of proteins used in *in vitro* tests may hamper the extrapolation of *in vitro* data to *in vivo* conditions.

Acknowledgements

This work is part of the Ph.D. research activity of one of the authors (AM). She has been financed by the Italian Ministry of Education, University and Research (MIUR). SEM inspections have been performed at Nanofacility Piemonte INRiM, a laboratory supported by Compagnia di San Paolo Foundation.

Declaration of interest statement

All authors declare they have no conflict of interests.

References

Barrán-Berdón AL, Pozzi D, Caracciolo G, Capriotti AL, Caruso G, Cavaliere C, Riccioli A, Palchetti S, Laganà A. 2013. Time evolution of nanoparticle−protein corona in human plasma: relevance for targeted drug delivery. Langmuir 29 6485−6494.

Deng Z J, Liang M T., Monteiro M, Toth I, Minchin RF. 2011.Nanoparticle-induced unfolding of fibrinogen promotes Mac-1 receptor activation and inflammation. Nat. Nanotechnol. 6 (1): 39-44.

Deng Z J, Mortimer G, Schiller T, Musumeci A, Martin D, Minchin R. 2009. Differential plasma protein binding to metal oxide nanoparticles. Nanotechnology 20 (45).

Doolittle R F. 2003. X-ray crystallographic studies on fibrinogen and fibrin. J. Thromb. Haemost. 1 (7): 1559-1565

Engberg AE, Rosengren-Holmberg JP, Chen H, Nilsson B, Lambris JD, Nicholls IA, Ekdahl KN. 2012 Blood protein-polymer adsorption: Implications for understanding complement-mediated hemoincompatibility J. Biomed. Mater. Res. A, 97A (1) 74-84.

Erdem B, Hunsicker R A, Simmons G W, Sudol E D, V L Dimonie, El-Aasser MS 2001. XPS and FTIR surface characterization of TiO_2 particles used in polymer encapsulation. Langmuir 17 (9): 2664-2669

Fenoglio I, Fubini B, Ghibaudi E M, Turci F. 2011. Multiple aspects of the interaction of biomacromolecules with inorganic surfaces. Adv. Drug Deliv. Rev. 63 (13): 1186-1209.

Fuss C, Palmaz JC, Sprague EA. 2001. Fibrinogen: Structure, function, and surface interactions. J. Vasc. Interv. Radiol. 12 (6): 677-682.

Galisteo F, and Norde W. 1995. Protein adsorption at the agi-water interface. J. Coll. Inter. Sci. 172 (2): 502-509.

Gerloff K, Fenoglio I, Carella E, Kolling J, Albrecht C, Boots AW, Forster I, Schins R P F. 2012 Distinctive toxicity of TiO_2 Rutile/Anatase mixed phase nanoparticles on Caco-2 cells Chem. Res. Toxicol. 25 (3): 646-655.

Ghigo D, Aldieri E, Todde R, Costamagna C, Garbarino G, Pescarmona G, Bosia A. 1998 Chloroquine stimulates nitric oxide synthesis in murine, porcine, and human endothelial cells. J. Clin. Invest. 102, 595−605.

Guadiz G, Sporn L A, Goss R A, Lawrence S O, Marder V J, SimpsonHaidaris P J. 1997. Polarized secretion of fibrinogen by lung epithelial cells. Am. J. Respir. Cell Mol. Biol. 17 (1): 60-69.

Gunawan C, Lim M, Marquis CP, Amal R. 2014. Nanoparticle–protein corona complexes govern the biological fates and functions of nanoparticles J. Mater. Chem. B, 2: 2060- 2083.

Jackson S P. 2007. The growing complexity of platelet aggregation. Blood 109 (12): 5087-5095.

Jones C, Campbell R A, Brooks AE, Assemi S, Tadjiki Soheyl,Thiagarajan G, Mulcock C, Weyrich A S, Brooks BD, Ghandehari H and Grainger W. 2012. Cationic PAMAM dendrimers aggressively initiate blood clot formation. ACS Nano 6 (11): 9900-9910

Jung SY, Lim SM, Albertorio F, Kim G, Gurau MC, Yang RD, Holden MA, Cremer P S. 2003. The Vroman effect: A molecular level description of fibrinogen displacement. J. Am. Chem. Soc. 125 (42): 12782-12786.

Karmali P P, and Simberg D. 2011. Interactions of nanoparticles with plasma proteins: implication on clearance and toxicity of drug delivery systems. Expert Opin Drug Deliv 8 (3): 343-357.

Koo J, Rafailovich M H, Medved L, Tsurupa G, Kudryk B, Liu Y, Galanakis D. 2010. Evaluation of fibrinogen self-assembly: role of its alpha C region. Journal of Thrombosis and Haemostasis 8 (12): 2727-2735.

Lesniak A, Fenaroli F, Monopoli M R, Aberg C, Dawson K A, Salvati A. 2012. Effects of the presence or absence of a protein corona on silica nanoparticle uptake and impact on cells. ACS Nano 6 (7): 5845-5857.

Lishko VK, Kudryk B, Yakubenko VP, Yee VC, Ugarova TP. 2002. Regulated unmasking of the cryptic binding site for integrin alpha(M)beta(2) in the gamma C-domain of fibrinogen. Biochemistry 41(43):12942-12951.

Lynch I, Cedervall T, Lundqvist M, Cabaleiro-Lago C, Linse S, Dawson KA. 2007. The nanoparticle - protein complex as a biological entity; a complex fluids and surface science challenge for the 21st century, Adv. Colloid Interface Sci. 134-35: 167-174.

Lynch I, Dawson KA. 2008. Protein–nanoparticle interactions. Nano Today 3:40–47.
Lundqvist M, Stigler J, Elia J, Lynch I, Cedervall T, Dawson KA. 2008. Nanoparticle size and surface properties determine the protein corona with possible implications for biological impacts PNAS. 38: 14265–14270.
Mao H, Chena W, Laurent S, Thirifays C, Burtea C, Rezaeed F, Mahmoudie M. 2013. Hard corona composition and cellular toxicities of the graphene sheets Coll. Surf. B: Biointerfaces 109:212– 218.
Marder. 1982. Fibrinogen structure and physiology, JB Lippincott Co.
Marucco A, Fenoglio I, Turci F, Fubini B. Iop, 2013 Interaction of fibrinogen and albumin with titanium dioxide nanoparticles of different crystalline phases, Nanosafe 2012: International Conferences on Safe Production and Use of Nanomaterials 429:10.
Marucco A, Turci F, O'Neill L, Byrne H J, Fubini B, Fenoglio I. 2014. Hydroxyl density affects the interaction of fibrinogen with silica nanoparticles at physiological concentration. J. Coll. Interface Sci. 419: 86-94.
Mathias J, Wannemacher GJ. 1988. Basic characteristics and applications of aerosil:30. The chemistry and physics of the aerosil Surface. Colloid Interface Sci. 125: 61–68.
Mbawuike IN, and Herscowitz B. 1989. MH-S, a murine alveolar macrophage cell-line - morphological, cytochemical, and functional-characteristics. J. Leukoc. Biol. 46(2): 119-127.
Monteiro NA, Samberg ME, Oldenburg SJ, Riviere JE. 2013. Protein binding modulates the cellular uptake of silver nanoparticles into human cells: Implications for in vitro to in vivo extrapolations? Toxicol. Lett. 220:286– 293.
Mortensen NP, Hurst GB, Wang W, Foster CM, Nallathamby PD, Retterer ST. 2013.Dynamic development of the protein corona on silica nanoparticles: composition and role in toxicity. Nanoscale 5 (14): 6372-6380.
Nagayama S, Ogawara K, Fukuoka Y, Higaki K, Kimura T 2007 Time-dependent changes in opsonin amount associated on nanoparticles alter their hepatic uptake characteristics Int. J. Pharmac. 342: 215–221.
Norde W. 2008. My voyage of discovery to proteins in flatland…and beyond, Colloids and Surfaces. B, Biointerfaces 61:1–9.
Oberdorster G, Maynard A, Donaldson K, Castranova V, Fitzpatrick J, Ausman K, Carter J, Karn B, Kreyling W, Lai D, Olin S, Monteiro-Riviere N, Warheit D, Yang H. 2005. Screening working, principles for characterizing the potential human health effects from exposure to nanomaterials: elements of a screening strategy. Part. Fibre Toxicol. 2: 8-8
Owens III DA, Peppas NA. 2006. Opsonization, biodistribution, and pharmacokinetics of polymeric nanoparticles. Int. J. Pharmaceut. 307:93–102.
Pery ARR, Brochot C, Hoet PHM, Nemmar A, Bois FY. 2009. Development of a physiologically based kinec model for 99m-Technetium-labelled carbon nanoparticles inhaled by humans. Inhal.Toxicol. 21 (13) 1099-1107.
Polimeni M, Gazzano E, Ghiazza M, Fenoglio I, Bosia A, Fubini B, Ghigo D. 2008 Quartz inhibits glucose 6-phosphate dehydrogenase in murine alveolar macrophages. Chem Res Toxicol 21(4):888-94.
Plow E F, and Hoover-Plow J. 2004. The functions of plasminogen in cardiovascular disease. Trends Cardiovasc. Med. 14(5):180-186.
Pozzi D, Colapicchioni V, Caracciolo G, Piovesana S, Capriotti AL, Palchetti S, De Grossi S, Riccioli A, Amenitsch E, Laganà A. 2014. Effect of polyethyleneglycol (PEG) chain length on the bio–nano-interactions between PEGylated lipid nanoparticles and biological fluids: from nanostructure to uptake in cancer cells. Nanoscale. 6: 2782-2792
Prokop A and Davinson J M. 2008.Nanovehicular intracellular delivery systems. J. Pharm. Sci. 97 (9): 3518-3590.
Rezwan K, Studart AR, Voros J, Gauckler L J. 2005. Change of xi potential of biocompatible colloidal oxide particles upon adsorption of bovine serum albumin and lysozyme, J. Phys. Chem. B 109 14469-14474.
Ruh H, Kuhl B, Brenner-Weiss G, Hopf C, Diabate S, Weiss C, 2012. Identification of serum proteins bound to industrial nanomaterials Toxicol. Lett. 41–50.
Savolainen K, Pylkkanen L, Norppa H, Falck G, Lindberg H, Tuomi T, Vippola M, Alenius H, Hameri K, Koivisto J, Brouwer D, Mark D, Bard D, Berges M, Jankowska E, Posniak M, Farmer P, Singh R, Krombach F, Bihari P, Kasper G, Seipenbusch M. 2010.Nanotechnologies, engineered nanomaterials and occupational health and safety - A review. Safety Science 48 (8) 957-963.

Schrurs F and Lison D. 2012. Focusing the research effort. Nat. Nanotechnol. 7(9): 546-548.
Tang L P, 1998 Mechanisms of fibrinogen domains: biomaterial interactions, J. Biomater. Sci.-Polym. Ed. 9 (12): 1257-1266.
Tenzer S, Docter D, Kuharev J, Musyanovych A, Fetz V, Hecht R, Schlenk F, Fischer D, Kiouptsi K, Reinhardt C, Landfester K, Schild H, Maskos M, Knauer SK, Stauber RH. 2013. Rapid formation of the plasma protein corona critically affects nanoparticle pathophysiology Nat. Nanotechnol. 8: 772-781.
Thevenot P, Hu WJ, Tang LP. 2008. Surface chemistry influences implant biocompatibility, Curr. Top. Med. Chem. 8:270–280.
Tsurupa G, Hantgan R R, Burton R A, Pechik I, Tjandra N, Medved L. 2009. Structure, Stability, and interaction of the fibrin(ogen) alpha C-Domains, Biochemistry 48 (51): 12191-12201.
Tsurupa G, Medved L, 2001. Identification and characterization of novel tPA- and plasminogen-binding sites within fibrin(ogen) alpha C-domains. Biochemistry 40(3): 801-808.
Turci F, Ghibaudi E, Colonna M, Boscolo B, Fenoglio I, Fubini B. 2010. An integrated approach to the study of the interaction between proteins and nanoparticles. Langmuir 26 (11) 8336-8346.
Vilaseca P, Dawson K A, Franzese G. 2013. Understanding and modulating the competitive surface-adsorption of proteins through coarse-grained molecular dynamics simulations. Soft Matter 9 (29):6978-6985
Vroman L. 1962. Effect of absorbed proteins on the wettability of hydrophilic and hydrophobic solids. Nature 196: 476-477.
Wertz CF, Santore MM. 2002. Fibrinogen adsorption on hydrophilic and hydrophobic surfaces: geometrical and energetic aspects of interfacial relaxations. Langmuir 18:706-715.

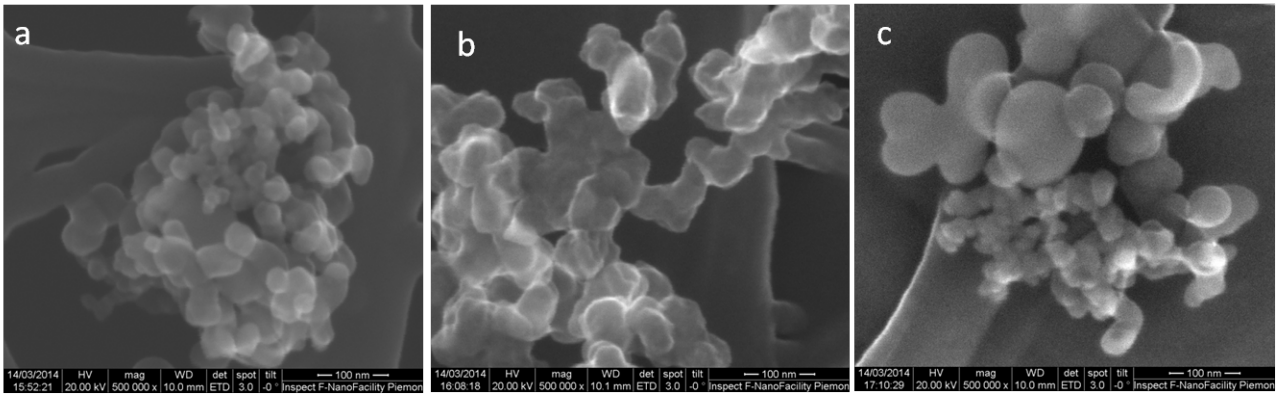

Figure 1 SEM micrographs of the NMs. The images of a) NM-TiO_2; b) NM-C; and c) NM-SiO_2; show that the samples are composed by aggregates of nanoparticles. A roughness is observed for the particles of NM-C.

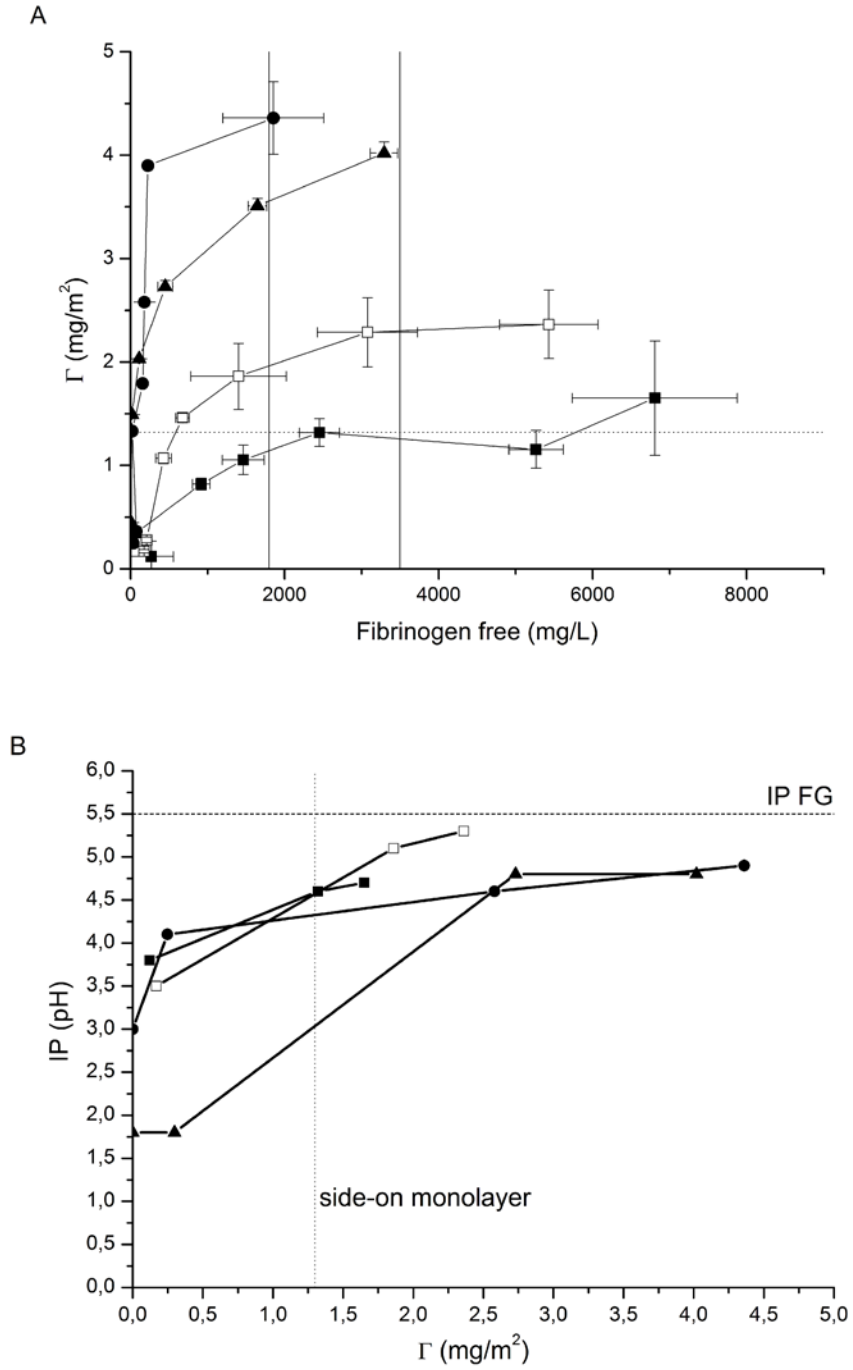

Figure 2 A) Adsorption isotherms of fibrinogen on NMs. The amount of fibrinogen interacting with the NM is expressed as amount per unit surface area *vs* the final concentration of protein in the supernatant. The horizontal line indicates the amount of FG adsorbed to build up a theoretical side-on monolayer on a flat surface. The vertical lines indicate the range of physiological concentration of FG; B) IP shift induced by FG adsorption. The horizontal line indicates the IP of FG. (●) NM-SiO_2, (▲) NM-TiO_2, (■) NM-C (1 h) and (□) NM-C (24 h).

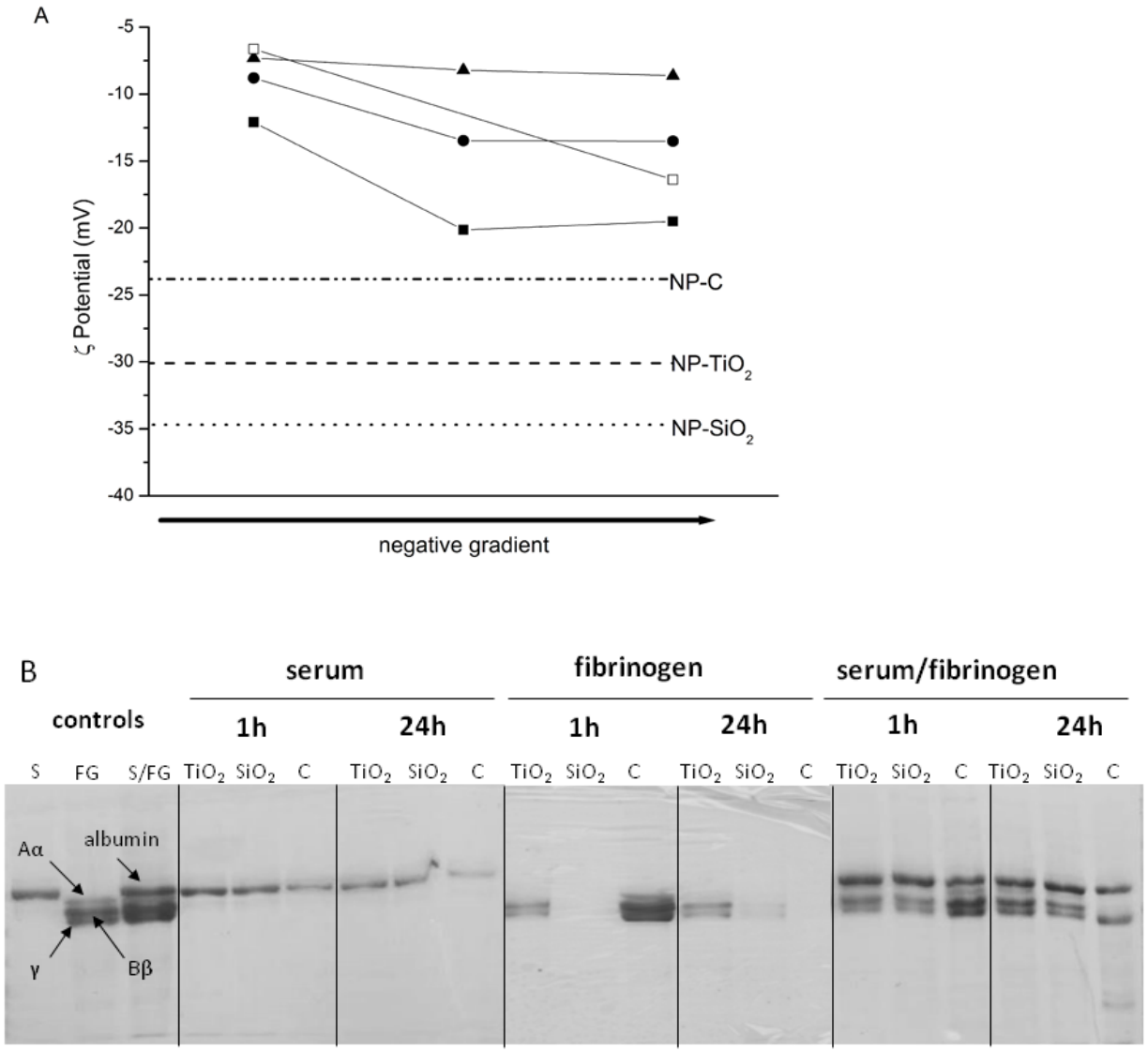

Figure 3 A) Strength of FG/ NMs interaction. ζ- potential shift (pH 7.4) following washing of the NMs/FG conjugates prepared at a fibrinogen concentration of 5 g/l. (●) NM-SiO_2, (▲) NM-TiO_2, (■) NM-C (1 h) and (□) NM-C (24 h). The horizontal lines indicate the PZC of the NMs. B) Competitive interaction of fibrinogen and serum proteins with SiO_2, TiO_2 and carbon NMs. SDS-PAGE separation of the proteins of the supernatant after incubation of the NMs with a solution of FG (3.5 g/l), serum proteins (0.8 g/l) and a mixture of both for 1 and 24 h. The control solutions have been diluted 1:2 prior deposition.

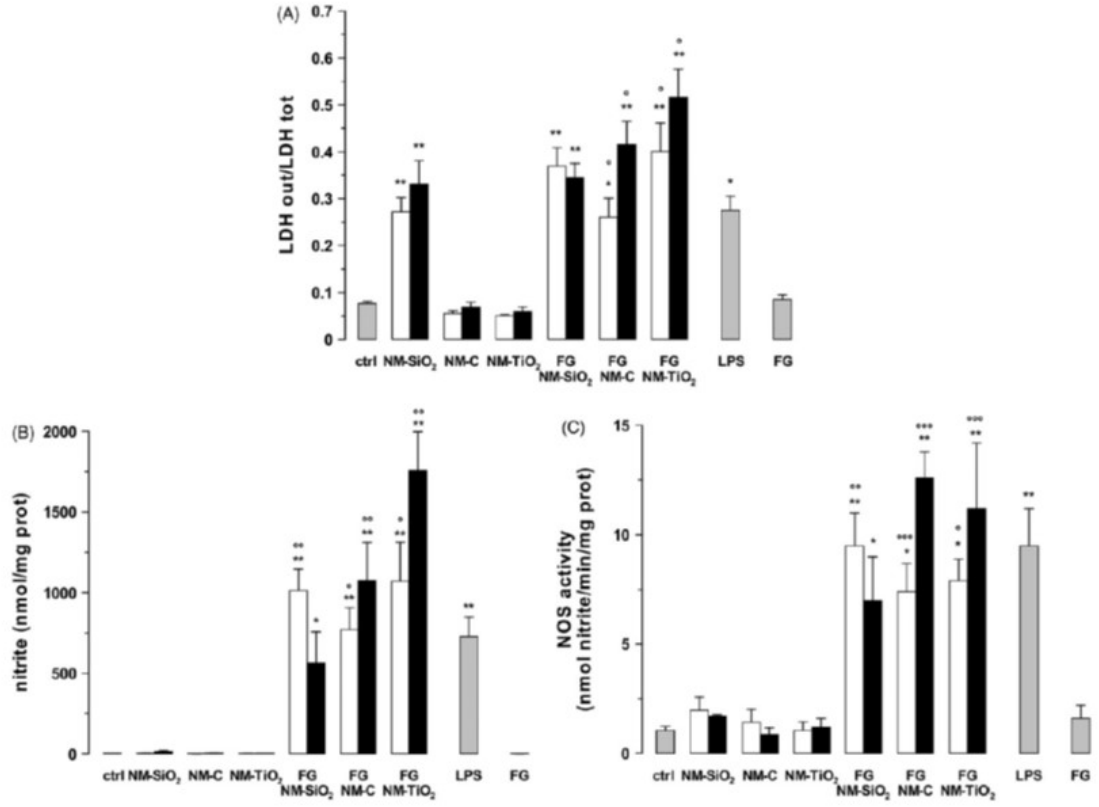

Figure 4 The MH-S cells were incubated for 24 h in the absence of stimuli (ctrl), with FG alone (1 mg/l), lipopolysaccharide alone (LPS, 0.01 μg/ml, positive control) (all indicated with grey bars), 10 μg/ml NMs (white bars) and 50 μg/ml NMs (black bars), alone or pre-incubated with a 10 g/l solution of FG. A) Cell viability measured as release of LDH into the extracellular medium; B) NO release as extracellular nitrite; C) activation of intracellular NO synthase. Significance: A) *p < 0.004, **p < 0.0001 vs ctrl; °p < 0.0001 vs pristine NMs. B) *p < 0.04, **p < 0.0001 vs ctrl; °p < 0.001, °°p < 0.0001 vs pristine NMs. C) *p < 0.005, **p < 0.0001 vs ctrl; °p < 0.02, °°p < 0.003, °°°p < 0.0001 vs pristine NMs.

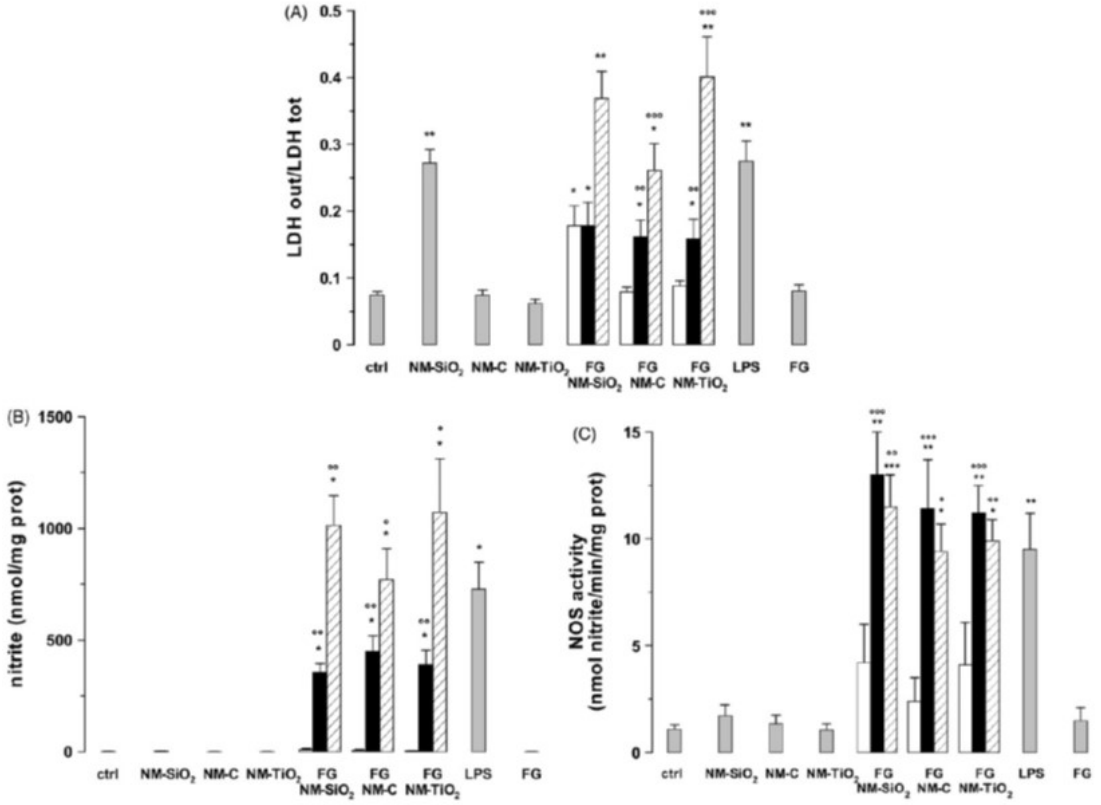

Figure 5 The MH-S cells were incubated for 24 h in the absence of stimuli (ctrl), with NMs alone (10 μg/ml), FG alone (1 mg/l) and lipopolysaccharide alone (LPS, 0.01 μg/ml, positive control) (all indicated with grey bars) or NMs pre-incubated with FG at different concentrations (white bars: 0.75 g/l; black bars: 3.5 g/l; dashed bars: 10 g/l). A) Cell viability measured as release of LDH into the extracellular medium; B) NO release as extracellular nitrite; C) activation of intracellular NO synthase. Significance: A, B) * $p < 0.05$; ** $p < 0.001$ vs ctrl; C) * $p < 0.05$, ** $p < 0.001$ vs ctrl; ° $p < 0.0001$ vs pristine NMs.

Table 1. Main physico-chemical properties of the nanomaterials [a]

sample	Composition (%wt)	SSA[f] (m^2/g)	Primary particle size (nm)	Abundance of acidic surface functionalities (number/nm^2)	ζ potential (pH7.4, PBS) (mV)	PZC (pH)
NM-TiO_2	TiO_2> 99.0[b]	52.6±0.1[c]	31.3±9.8	2.2 (SiOH)[d]	-30	1.8
NM-C	nd	58.1±0.2	nd	0.24 (-COOH)	-23	<2
NM-SiO_2	SiO_2> 99.5[b]	56.4±0.4	38.5± 8.7	3.3 (Ti-OH)[e]	-35	3.0

[a]abbreviations: SSA specific surface area; PZC point of zero charge; [b] as declared by the supplier, [c] Gerloff et al 2012; [d] Mathias and Wannemacher 1988; [e] Erdem et al. 2001